Mendeleev Communications

Mendeleev Commun., 2025, **35**, 193–195

$CsPbBr_3$ and Cs_4PbBr_6 perovskite nanoparticles: hidden potential of Cs_4PbBr_6 or ineffective fluorescence?

Alexandra G. Son,*[a] Valeria A. Gushchina,[a] Anastasia A. Egorova,[a] Alexey A. Sadovnikov,[a] Nikolay A. Bert[b], Alexey R. Tameev[c] and Sergey A. Kozyukhin[a]

[a] *N. S. Kurnakov Institute of General and Inorganic Chemistry, Russian Academy of Sciences, 119991 Moscow, Russian Federation. Fax: +7 495 952 0787; e-mail: sonsacha@gmail.com*
[b] *Ioffe Institute, 194021 St. Petersburg, Russian Federation*
[c] *A. N. Frumkin Institute of Physical Chemistry and Electrochemistry, Russian Academy of Sciences, 119071 Moscow, Russian Federation*

DOI: 10.71267/mencom.7612

All-inorganic perovskite $CsPbBr_3$ and Cs_4PbBr_6 nanoparticles are intensively studied for their unique optical properties, though synthesizing single-phase nanoparticles has posed challenges. Detailed synthesis method of $CsPbBr_3$ and Cs_4PbBr_6 single-phase nanoparticles and their chemical and phase analysis are described. Distinctive optical characteristics, such as photoluminescence, optical band gap and the Urbach tail region, are revealed and explained within the current conception of perovskite band structures.

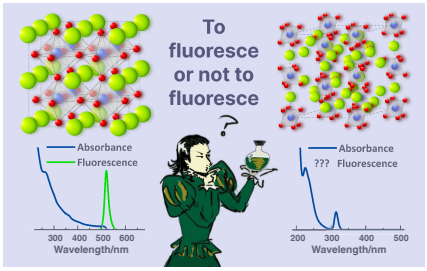

Keywords: perovskite, Cs_4PbBr_6, $CsPbBr_3$, nanoparticles, luminescence, optical absorbance.

Hybrid organic-inorganic materials with the ABX_3 perovskite structure, where A is an organic or inorganic cation, B is lead and X is a halogen, are of great importance in the development of next generation optoelectronic devices, such as solar cells, LEDs and photodetectors, due to their distinctive optical and electronic properties. These properties include a high absorption coefficient, low exciton binding energy, band gap sensing capability,[1] high charge carrier mobility and low defect density.[2–6] Over the last decade, a marked improvement of the perovskite solar cells efficiency, from 3.8 to 26.1%, has been achieved. Additionally, a perovskite/silicon solar cells pair have demonstrated the efficiency of approximately 34.6%.[7,8] One of the problems of hybrid perovskites is their instability and degradation of properties, which are caused by the presence of an organic cation in the structure. In contrast, inorganic perovskites containing Cs^+ instead of organic cations show improved stability.[9] $CsPbX_3$ nanoparticles (NPs) possess a number of advantages over other NPs, including a wide absorption spectrum, bright photoluminescence, a long diffusion path length for photoexcited carriers and tunable emission properties.[10,11] However, the stability of perovskite devices is a challenge in real-world conditions due to the high chemical activity and ionic nature of these materials, particularly in the presence of polar solvents.[12] Nevertheless, perovskite nanocrystals remain a promising area of research in photovoltaics. The CsX–PbX_2 phase diagram encompasses a range of thermodynamically stable compounds, including Cs_4PbX_6 and $CsPbX_3$.[13] Nanocrystals of $CsPbBr_3$ exhibit bright green emission and a high luminescence quantum yield (~92.8%),[14] whereas the luminescent properties of Cs_4PbBr_6 NPs remain poorly understood.[10] Unsufficient study of Cs_4PbBr_6 NPs can be caused by the difficulty of obtaing pure particles of this composition.[15] Synthesis of mixed compositions of $CsPbBr_3$ and Cs_4PbBr_6 was described earlier.[16,17] It was also expected, that $CsPbBr_3$ structure could undergo a transition into Cs_4PbBr_6 when a substantial quantity of stabilizers was incorporated into the colloidal solution[18–20] or upon the introduction of $ZnBr_2$.[21] As there is currently no general agreement on the luminescent properties of the compound, various models have been proposed by different research groups. It has been demonstrated in several works on the preparation of Cs_4PbBr_6 nanocrystals that this type of perovskite does not exhibit luminescence.[18,19,21] On the other hand, some studies posit that luminescence may be enabled by the existence of intrinsic defects, namely halide vacancies, within the Cs_4PbBr_6 crystal structure. However, this hypothesis has yet to be validated through empirical research.[22,23,24] The aim of our study was to synthesize Cs_4PbBr_6 NPs devoid of any $CsPbBr_3$ contaminants *via* simple approach and to analyze the optical properties of the resulting NP colloidal solutions, with particular emphasis on the nature of the Cs_4PbBr_6 luminescence.

The perovskite nanoparticles were obtained *via* two distinct methodological approaches: the hot injection method[11,25] and the ultrasonic treatment method.[26] $CsPbBr_3$ NPs (henceforth referred to as 113 HI) were synthesized through the injection of cesium oleate into a solution of lead bromide in a non-coordinating, high-boiling solvent, with the addition of a modest quantity of oleic acid, oleylamine, and pentadecylamine. Cs_4PbBr_6 NPs (416) were obtained through the application of the ultrasonic treatment (UT) at room temperature and under ambient conditions. The precursors of cesium carbonate and lead bromide in a ratio of 4 : 1 by molar weight, along with stabilizers oleic acid, oleylamine and pentadecylamine, were dispersed in mineral oil using an ultrasonic homogenizer. Excess of Cs^+ ions would occupy positions within the Cs lattice surrounding the $[PbBr_6]^4$ octahedron. As a result, the $[PbBr_6]^4$ octahedron, which originally shared Br atoms, is isolated by the additional Cs ions.[3] Furthermore, the synthesis of $CsPbBr_3$ was carried out using

ultrasonic treatment (hereinafter 113 UT), with 1 : 1 ratio of cesium carbonate to lead bromide in the precursor. Subsequently, the colloidal solutions were subjected to centrifugation, then the precipitate was dispersed in a low-boiling solvent, particularly *n*-hexane.

Figure 1(*a*) depicts the X-ray diffraction (XRD) patterns of the perovskite NPs. The $CsPbBr_3$ sample synthesized *via* the hot injection method (curve *1*) exhibits a cubic phase belonging to the *Pm-3m* group (PDF2 #54-0752). According to the XRD data, the Cs_4PbBr_6 NPs (curve *3*) are adequately described by the rhombohedral Cs_4PbBr_6 structure, which belongs to the *R-3c* group (PDF2 #73-2478). XRD analyses indicate that both types of nanoparticles possess high crystal quality, exhibiting no evidence of secondary phases. The lattice parameters and unit cell volumes for the samples were extracted from the data presented in Table S1 (see Online Supplementary Materials). The morphology of the perovskite nanoparticles was examined using scanning transmission electron microscopy (STEM) (see Figure S2 in Online Supplementary Materials) and transmission electron microscopy (TEM), as illustrated in Figure 1(*b*) and (*c*). The $CsPbBr_3$ sample (113 HI) is composed of cubic particles of 6–13 nm, while the Cs_4PbBr_6 sample (416 UT) exhibits cubic particles of 30–70 nm. A significant proportion of the particles display a central pore of approximate size 5 nm, with some particles exhibiting multiple pores. Notably, the STEM images of $CsPbBr_3$ (113 UT) obtained by ultrasonic treatment (see Figure S4) reveal the presence of particles of various sizes including 10–20 nm and larger (50–70 nm). The STEM images show that the 113UT sample contains a mixture of homogeneous particles, each particle possessing a single phase. The images clearly indicate that there is no mixing of phases within individual nanoparticles; the sample rather consists of particles each corresponding to a single, pure phase. This confirms that the 113UT synthesis method yields a colloidal solution containing separate populations of single-phase nanoparticles, rather than individual nanoparticles with multiple phases. These nanoparticles exhibit a distinct XRD pattern (curve 2) suggestive of the formation of two distinct phases, 113 and 416, which is corroborated by the observed absorbance spectra.

Figure 2 shows the absorption and normalized luminescence spectra of the synthesized colloidal solutions of perovskite NPs. The $CsPbBr_3$ (113 HI) absorption spectrum [Figure 2(*a*), curve *1*] comprises multiple maxima, whose positions correlate with the wavelengths 225, 260, 360 and 510 nm.[25] This 113 HI sample exhibits bright fluorescence with an emission center at a wavelength of 518 nm [Figure 2(*b*), curve *1*]. The absorption spectrum of the sample 416 [Figure 2(*a*), curve *3*] is distinguished by the presence of two maxima at 225 nm and 313 nm.[3] The absorption band at 313 nm is attributed to the localized $^6S_{1/2} \rightarrow {}^6P_{1/2}$ transition inside individual $[PbBr_6]^{4-}$ octahedra separated by Cs^+ ions, corresponding to the absorption edge of Cs_4PbBr_6 NPs.[21,27] Liu *et al*. found that absorption band position remained unaltered relative to the NP size, thereby corroborating the hypothesis concerning the isolation of $[PbBr_6]^{4-}$ octahedra from one another within Cs_4PbBr_6 NPs.[22] A colloidal solution of NPs does not exhibit visible light absorption, which is consistent with findings reported previously for Cs_4PbBr_6 NPs, as well as for crystals and thin films of this composition.[19,21] An identical maximum was observed in the absorption spectrum of the Cs_4PbCl_6 crystal. S. Kondo *et al*. attributed this phenomenon to the absorption of cesium ions.[27] Fluorescence was not observed in the sample 416 [Figure 2(*b*), curve *3*], which indicates the absence of emission centers. This result is consistent with earlier reports.[19,21] The absorption spectrum of the $CsPbBr_3$ (113 UT) composition synthesized by ultrasonic treatment exhibits maxima identical to those observed in the 113 HI sample.

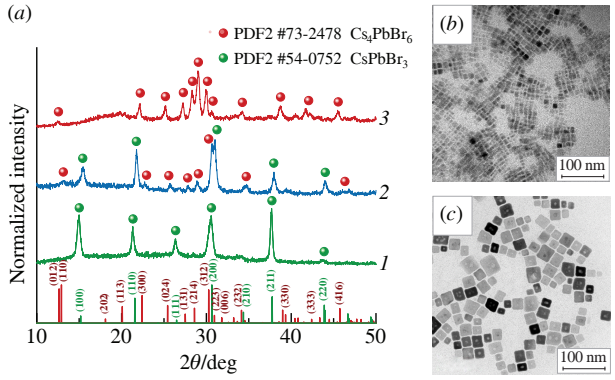

Figure 1 NPs XRD patterns (*a*): (*1*) – 113 HI, (*2*) – 113 UT, (*3*) – 416. TEM-image of perovskite NPs (*b*) $CsPbBr_3$ and (*c*) Cs_4PbBr_6.

However, an additional absorption band at 313 nm emerges, which is also present in the absorption spectra of the Cs_4PbBr_6 phase. The obtained particles also exhibit luminescence with a maximum at 518 nm, similar to that observed in particles obtained by hot injection. Based on the analysis of X-ray diffraction and absorption spectra, it can be concluded that two-phase particles have been formed during synthesis *via* ultrasonic treatment. The data raise the question why luminescence is not found in the pure Cs_4PbBr_6. The fundamental parameter that defines the applicability of a material as a light absorbing layer for photoelectric devices is the optical band gap, denoted as E_g. To estimate this value from the experimental optical absorption spectra, the Tauc method has been employed – it describes the dependence of the absorbance of a direct-gap semiconductor *vs.* the photon energy.[28]

Based on the results of UV-VIS spectrophotometry for the NP samples 113 HI and 416, the band gap values were determined as 2.34 ± 0.05 and 3.73 ± 0.05 eV, respectively (see Figures S6 and S7). The absorption spectra of sample 113 UT revealed the presence of the maxima, indicative of the coexistence of two types of particles, $CsPbBr_3$ and Cs_4PbBr_6, in the colloidal solution. Therefore, the estimated band gap width for both phases comprises 2.38 ± 0.05 and 3.77 ± 0.05 eV, respectively (see Figure S8).

It is established that perovskites have a high density of localized states in the band gap that are described by Urbach law.[29,30] It is also known that in perovskite structures, when a free electron couples with a hole, an exciton may be formed, which is highly likely to dissociate again into a free electron and hole. In turn, free electrons and holes can recombine either radiatively, causing photoluminescence, or non-radiatively. The area of exponential change in the absorbance with increasing photon energy is called the Urbach tail, and it appears in low-crystalline, poorly crystalline, disordered and amorphous materials because these materials have localized tail states that extend into the band gap.[31] The value of Urbach energy (E_U) can

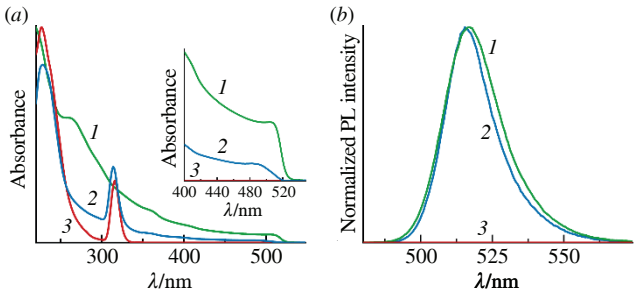

Figure 2 (*a*) Absorption spectra and (*b*) normalized emission spectra (λ_{exc} = 260 nm) of the perovskite NPs: (*1*) – 113 HI, (*2*) – 113 UT, (*3*) – 416. Inset: absorption spectra in the weak absorption region.

be defined as the minimum possible for a sample without defects.[32–34] According to the approximation of the absorption spectra performed in our work, the E_U values are 7.3 and 190.1 meV for $CsPbBr_3$ and Cs_4PbBr_6 NPs, respectively (see Figure S9 and Figure S10). It can be assumed that in Cs_4PbBr_6 NPs electrons and holes remain as free charges much longer than as bound excitons, and therefore free electrons are more susceptible to capture at defect sites of large density, that results in nonradiative decay. If the density of defect states is reduced, as in the $CsPbBr_3$ NPs with low Urbach energy, the charge carriers remain as excitons for a longer time, and radiative recombination occurs during their dissociation. Hence, the probability of radiative decay increases relative to the charge trapping, that is expressed in the bright green emission.

In summary, modified methods of hot injection and UT were employed to obtain colloidal solutions of Cs_4PbBr_6 and $CsPbBr_3$ perovskite NPs. The optical band gaps were estimated as 2.34 ± 0.05 eV for 113 HI, 3.73 ± 0.05 eV for 416 and two values, 3.77 ± 0.05 eV and 2.38 ± 0.05 eV for 113 UT. $CsPbBr_3$ exhibited bright luminescence with an emission maximum at 518 nm, whereas Cs_4PbBr_6 showed no emission in UV and visible spectral ranges. The Urbach tail energy analysis revealed a higher density of defect states in Cs_4PbBr_6 compared with $CsPbBr_3$. Notably, the lower Urbach energy in the 113 UT NPs correlated with reduced defect states, longer exciton lifetime and enhanced luminescence. These findings provide valuable insights into the optical and defect-related properties of inorganic perovskites for optoelectronic applications.

The study was supported by the Russian Science Foundation (project no. 23-19-00884) and was performed using the equipment of the JRC PMR IGIC RAS.

Online Supplementary Materials

Supplementary data associated with this article can be found in the online version at doi: 10.71267/mencom.7612.

References

1 S. A. Fateev, A. D. Riabova, E. A. Goodilin and A. B. Tarasov, *Mendeleev Commun.*, 2023, **33**, 311; https://doi.org/10.1016/j.mencom.2023.04.004.

2 E. M. Nemygina, N. N. Udalova, E. I. Marchenko, A. K. Moskalenko, E. A. Goodilin and A. B. Tarasov, *Mendeleev Commun*., 2024, **34**, 660; https://doi.org/10.1016/j.mencom.2024.09.011.

3 J. Zhang, G. Hodes, Z. Jin, S. Liu and S. Liu, *Angew. Chem., Int. Ed.*, 2019, **58**, 15596; https://doi.org/10.1002/anie.201901081.

4 F. Chen, L. Xu, Y. Li, T. Fang, T. Wang, M. Salerno, M. Prato and J. Song, *J. Mater. Chem. C*, 2020, **8**, 13445; https://doi.org/10.1039/D0TC03042B.

5 Y. He, M. Petryk, Z. Liu, D. G. Chica, I. Hadar, C. Leak, W. Ke, I. Spanopoulos, W. Lin, D. Y. Chung, B. W. Wessels, Z. He and M. G. Kanatzidis, *Nat. Photonics*, 2021, **15**, 36; https://doi.org/10.1038/s41566-020-00727-1.

6 Y. Zhang, A. Kirs, F. Ambroz, C.-T. Lin, A. S. R. Bati, I. P. Parkin, J. G. Shapter, M. Batmunkh and T. J. Macdonald, *Small Methods*, 2021, **5**, 2000744; https://doi.org/10.1002/smtd.202000744.

7 M. A. Green, E. D. Dunlop, M. Yoshita, N. Kopidakis, K. Bothe, G. Siefer, X. Hao and J.-Y. Jiang, *Prog. Photovoltaics*, 2025, **33**, 3; https://doi.org/10.1002/pip.3867.

8 [dataset] NREL, *Best Research-Cell Efficiency Chart*, 2024; https://www.nrel.gov/pv/cell-efficiency.html.

9 X. Meng, X. Tian, S. Zhang, J. Zhou, Y. Zhang, Z. Liu and W. Chen, *Sol. RRL*, 2022, **6**, 2200280; https://doi.org/10.1002/solr.202200280.

10 H. J. Snaith, *Nat. Mater.*, 2018, **17**, 372; https://doi.org/10.1038/s41563-018-0071-z.

11 L. Protesescu, S. Yakunin, M. I. Bodnarchuk, F. Krieg, R. Caputo, C. H. Hendon, R. X. Yang, A. Walsh and M. V. Kovalenko, *Nano Lett.*, 2015, **15**, 3692; https://doi.org/10.1021/nl5048779.

12 Y. Kim, E. Yassitepe, O. Voznyy, R. Comin, G. Walters, X. Gong, P. Kanjanaboos, A. F. Nogueira and E. H. Sargent, *ACS Appl. Mater. Interfaces*, 2015, **7**, 25007; https://doi.org/10.1021/acsami.5b09084.

13 J. Yin, P. Maity, M. de Bastiani, I. Dursun, O. M. Bakr, J.-L. Brédas and O. F. Mohammed, *Sci. Adv*., 2017, **3**, e1701793; https://doi.org/10.1126/sciadv.1701793.

14 Y. Li, M. Cai, M. Shen, Y. Cai and R.-J. Xie, *J. Mater. Chem. C*, 2022, **10**, 8356; https://doi.org/10.1039/D2TC01144A.

15 J. Hui, Y. Jiang, Ö. Ö Gökçinar, J. Tang, Q. Yu, M. Zhang and K. Yu, *Chem. Mater.*, 2020, **32**, 4574; https://doi.org/10.1021/acs.chemmater.0c00661.

16 F. Cao, D. Yu, W. Ma, X. Xu, B. Cai, Y. M. Yang, S. Liu, L. He, Y. Ke, S. Lan, K.-L. Choy and H. Zeng, *ACS Nano*, 2020, **14**, 5183; https://doi.org/10.1021/acsnano.9b06114.

17 Z. Bao, H.-D. Chiu, W. Wang, Q. Su, T. Yamada, Y.-C. Chang, S. Chen, Y. Kanemitsu, R.-J. Chung and R.-S. Liu, *J. Phys. Chem. Lett.*, 2020, **11**, 10196; https://doi.org/10.1021/acs.jpclett.0c03142.

18 Q. A. Akkerman, S. Park, E. Radicchi, F. Nunzi, E. Mosconi, F. De Angelis, R. Brescia, P. Rastogi, M. Prato and L. Manna, *Nano Lett.*, 2017, **17**, 1924; https://doi.org/10.1021/acs.nanolett.6b05262.

19 Z. Liu, Y. Bekenstein, X. Ye, S. C. Nguyen, J. Swabeck, D. Zhang, S.-T. Lee, P. Yang, W. Ma and A. P. Alivisatos, *J. Am. Chem. Soc*., 2017, **139**, 5309; https://doi.org/10.1021/jacs.7b01409.

20 H. Tian, Y. Liu and F.-L. Jiang, *Chem. Mater*., 2024, **36**, 8949; https://doi.org/10.1021/acs.chemmater.4c02018.

21 S. Sun, M. Lu, J. Guo, F. Zhang, P. Lu, Y. Fu, X. Bai, Z. Shi, Z. Wu, W. Yu and Y. Zhang, *Chem. Eng. J.*, 2022, **433**, 133556; https://doi.org/10.1016/j.cej.2021.133556.

22 M. I. Saidaminov, J. Almutlaq, S. Sarmah, I. Dursun, A. A. Zhumekenov, R. Begum, J. Pan, N. Cho, O. F. Mohammed and O. M. Bakr, *ACS Energy Lett*., 2016, **1**, 840; https://doi.org/10.1021/acsenergylett.6b00396.

23 S. Seth and A. Samanta, *J. Phys. Chem. Lett*., 2018, **9**, 176; https://doi.org/10.1021/acs.jpclett.7b02931.

24 Y.-K. Jung, J. Calbo, J.-S. Park, L. D. Whalley, S. Kim and A. Walsh, *J. Mater. Chem. A*, 2019, **7**, 20254; https://doi.org/10.1039/C9TA06874K.

25 V. A. Gushchina, A. G. Son, A. A. Egorova, A. A. Arkhipenko, M. A. Teplonogova, N. N. Efimov and S. A. Kozyukhin, *Russ. J. Inorg. Chem.*, 2024; https://doi.org/10.1134/S0036023624600928.

26 Y. Tong, E. Bladt, M. F. Aygüler, A. Manzi, K. Z. Milowska, V. A. Hintermayr, P. Docampo, S. Bals, A. S. Urban, L. Polavarapu and J. Feldmann, *Angew. Chem., Int. Ed*., 2016, **55**, 13887; https://doi.org/10.1002/anie.201605909.

27 S. Kondo, K. Amaya, S. Higuchi, T. Saito, H. Asada and M. Ishikane, *Solid State Commun.*, 2001, **120**, 141; https://doi.org/10.1016/S0038-1098(01)00363-5.

28 J. Tauc and T. A. Scott, *Physics Today*, 1967, **20**, 105; https://doi.org/10.1063/1.3033945.

29 S. D. Stranks, V. M. Burlakov, T. Leijtens, J. M. Ball, A. Goriely and H. J. Snaith, *Phys. Rev. Appl.*, 2014, **2**, 034007; https://doi.org/10.1103/PhysRevApplied.2.034007.

30 Y. Yamada, T. Nakamura, M. Endo, A. Wakamiya and Y. Kanemitsu, *J. Am. Chem. Soc.*, 2014, **136**, 11610; https://doi.org/10.1021/ja506624n.

31 A. S. Hassanien and A. A. Akl, *Superlattices Microstruct.*, 2016, **89**, 153; https://doi.org/10.1016/j.spmi.2015.10.044.

32 D. Gau, I. Galain, I. Aguiar and R. Marotti, *ChemRxiv. Cambridge: Cambridge Open Engage*, 2022; https://doi.org/10.26434/chemrxiv-2022-3w06g.

33 S. Zeiske, O. J. Sandberg, N. Zarrabi, C. M. Wolff, M. Raoufi, F. Peña-Camargo, E. Gutierrez-Partida, P. Meredith, M. Stolterfoht and A. Armin, *J. Phys. Chem. Lett*., 2022, **13**, 7280; https://doi.org/10.1021/acs.jpclett.2c01652.

34 S. Singh, C. Li, F. Panzer, K. L. Narasimhan, A. Graeser, T. P. Gujar, A. Köhler, M. Thelakkat, S. Huettner and D. Kabra, *J. Phys. Chem. Lett.*, 2016, **7**, 3014; https://doi.org/10.1021/acs.jpclett.6b01207.

Received: 5th September 2024; Com. 24/7612